

In vitro binding assay

T7-tagged proteins were produced in *Escherichia coli* and partially purified by absorption onto T7-tag antibody agarose. S-tagged proteins were generated using rabbit reticulocyte lysate (TnT, Promega). *In vitro* translated proteins were diluted with 0.5 ml of T7-tag bind/wash buffer (4.29 mM Na₂HPO₄, 1.47 mM KH₂PO₄, 2.7 mM KCl, 137 mM NaCl, 0.1% Tween-20, 0.002% NaN₃, pH 7.3) in the presence of 1 × 'Complete EDTA-free' protease inhibitor cocktail (Boehringer Mannheim). S-tagged proteins were then added to the corresponding T7-tagged protein bound to the agarose beads in microfuge tubes. Samples were incubated with shaking for 1 h at 25 °C. The agarose beads were washed three times with 1 ml of T7-tag bind/wash buffer in the presence of 1 × Complete EDTA-free protease inhibitor cocktail. Bound proteins were released by boiling agarose beads in protein loading buffer. Proteins were separated using SDS-PAGE and transferred to polyvinylidene difluoride membrane. S-tagged proteins were visualized using S-protein-alkaline phosphatase conjugates (Novagen); T7-tagged proteins were visualized using T7-tag antibody-alkaline phosphatase conjugates (Novagen). Between 0.5 µg and 5 µg of T7-LAG-1 or T7-LAG-3 and about 100 ng of each of the S-tagged proteins were used in each assay.

Transcript analysis

The 5' end of the *lag-3* message was determined by RT-PCR using *lag-3* specific primers and a primer to the *trans*-splicing leader SL1. Two alternative 5' ends were obtained. The inferred transcripts are predicted to encode two proteins, LAG-3A and LAG-3B.

RNA interference

The RNAi effect should be limited to *lag-3* specifically, because this gene is unique in the *C. elegans* genome²⁸. The DNA template for *in vitro* transcription contained all of the coding sequence for LAG-3A and 86 nucleotides of the *lag-3* 3' untranslated region. To assay the postembryonic *lag-3* phenotype, L1 larvae were soaked in 1–3 µg µl⁻¹ of double stranded *lag-3* RNA for 48 h at 20 °C or 25 °C in M9 buffer (22 mM KH₂PO₄, 42 mM NaH₂PO₄, 85 mM NaCl, 1 mM MgSO₄) in the presence of *E. coli* (Absorbance 600 nm, 0.75–1.0). After soaking, animals were transferred to Petri dishes to continue development. To assay the embryonic *lag-3* phenotype, L4 animals were soaked in M9 containing 1 µg µl⁻¹ *lag-3* dsRNA overnight, then transferred to plates to lay eggs, using essentially a described method²⁹.

Subcellular localization

Generation of transgenic nematodes carrying HS-Myc-LAG-3, heat shock conditions and antibody detection was done essentially as described⁸, except a whole mount freeze cracking method was used for fixation of the worms³⁰.

Received 25 January; accepted 3 March 2000.

- Kimble, J. & Simpson, P. The LIN-12/Notch signalling pathway and its regulation. *Annu. Rev. Cell Dev. Biol.* **13**, 333–361 (1997).
- Artavanis-Tsakonas, S., Rand, M. D. & Lake, R. J. Notch signalling: cell fate control and signal integration in development. *Science* **284**, 770–776 (1999).
- Ellisen, L. W. *et al.* TAN-1, the human homolog of the *Drosophila Notch* gene, is broken by chromosomal translocations in T lymphoblastic neoplasms. *Cell* **66**, 649–661 (1991).
- Joutel, A. *et al.* Notch3 mutations in CADASIL, a hereditary adult-onset condition causing stroke and dementia. *Nature* **383**, 707–710 (1996).
- Schroeter, E. H., Kisslinger, J. A. & Kopan, R. Notch1 signalling requires ligand-induced proteolytic release of intracellular domain. *Nature* **393**, 382–386 (1998).
- Struhl, G. & Adachi, A. Nuclear access and action of Notch in *in vivo*. *Cell* **93**, 649–660 (1998).
- Lecourtois, M. & Schweisguth, F. Indirect evidence for Delta-dependent intracellular processing of notch in *Drosophila* embryos. *Curr. Biol.* **8**, 771–774 (1998).
- Roehl, H., Bosenberg, M., Belloch, R. & Kimble, J. Roles of the RAM and ANK domains in signalling by the *C. elegans* GLP-1 receptor. *EMBO J.* **15**, 7002–7012 (1996).
- Tamura, K. *et al.* Physical interaction between a novel domain of receptor Notch and the transcription factor RBP-Jk/Su(H). *Curr. Biol.* **5**, 1416–1423 (1995).
- Christensen, S., Kodoyianni, V., Bosenberg, M., Friedman, L. & Kimble, J. *lag-1*, a gene required for *lin-12* and *glp-1* signalling in *Caenorhabditis elegans*, is homologous to human CBF1 and *Drosophila* Su(H). *Development* **122**, 1373–1383 (1996).
- Roehl, H. & Kimble, J. Control of cell fate in *C. elegans* by a GLP-1 peptide consisting primarily of ankyrin repeats. *Nature* **364**, 632–635 (1993).
- Greenwald, I. & Seydoux, G. Analysis of gain-of-function mutations of the *lin-12* gene of *Caenorhabditis elegans*. *Nature* **346**, 197–199 (1990).
- Kodoyianni, V., Maine, E. M. & Kimble, J. Molecular basis of loss-of-function mutations in the *glp-1* gene of *Caenorhabditis elegans*. *Mol. Biol. Cell* **3**, 1199–1213 (1992).
- Mango, S. E., Maine, E. M. & Kimble, J. Carboxy-terminal truncation activates *glp-1* protein to specify vulval fates in *Caenorhabditis elegans*. *Nature* **352**, 811–815 (1991).
- Austin, J. & Kimble, J. *glp-1* is required in the germ line for regulation of the decision between mitosis and meiosis in *C. elegans*. *Cell* **51**, 589–599 (1987).
- Fire, A. *et al.* Potent and specific genetic interference by double-stranded RNA in *Caenorhabditis elegans*. *Nature* **391**, 806–811 (1998).
- Greenwald, I. S., Sternberg, P. W. & Horvitz, H. R. The *lin-12* locus specifies cell fates in *Caenorhabditis elegans*. *Cell* **34**, 435–444 (1983).
- Berry, L. W., Westlund, B. & Schedl, T. Germ-line tumor formation caused by activation of *glp-1*, a *Caenorhabditis elegans* member of the Notch family of receptors. *Development* **124**, 925–936 (1997).
- Mitchell, P. J. & Tjian, R. Transcriptional regulation in mammalian cells by sequence-specific DNA binding proteins. *Science* **245**, 371–378 (1989).
- Hicks, G. R. & Raikhel, N. Y. Protein import into the nucleus: an integrated view. *Annu. Rev. Cell Dev. Biol.* **11**, 155–188 (1995).

- Diederich, R. J., Matsuno, K., Hing, H. & Artavanis-Tsakonas, S. Cytosolic interaction between deltex and Notch ankyrin repeats implicates deltex in the Notch signalling pathway. *Development* **120**, 473–481 (1994).
- Kopan, R., Nye, J. S. & Weintraub, H. The intracellular domain of mouse Notch: a constitutively activated repressor of myogenesis directed at the basic helix-loop-helix region of MyoD. *Development* **120**, 2385–2396 (1994).
- Jarriault, S. *et al.* Signalling downstream of activated mammalian Notch. *Nature* **377**, 355–358 (1995).
- Kato, H. *et al.* Involvement of RBP-J in biological functions of mouse Notch1 and its derivatives. *Development* **124**, 4133–4141 (1997).
- Smoller, D. *et al.* The *Drosophila* neurogenic locus *mastermind* encodes a nuclear protein unusually rich in amino acid homopolymers. *Genes Dev.* **4**, 1688–1700 (1990).
- Bartel, P. L. & Fields, S. (eds) *The Yeast Two-Hybrid System* (Oxford Univ. Press, New York, 1997).
- Kraemer, B. *et al.* NANOS-3 and FBF proteins physically interact to control the sperm-oocyte switch in *Caenorhabditis elegans*. *Curr. Biol.* **9**, 1009–1018 (1999).
- The *C. elegans* Sequencing Consortium. Genome sequence of the nematode *C. elegans*: a platform for investigating biology. *Science* **282**, 2012–2018 (1998); erratum *ibid* **283**, 35 (1999); erratum *ibid* **283**, 2103 (1998).
- Subramaniam, K. & Seydoux, G. *nos-1* and *nos-2*, two genes related to *Drosophila nanos*, regulate primordial germ cell development and survival in *Caenorhabditis elegans*. *Development* **126**, 4861–4871 (1999).
- Crittenden, S. L. & Kimble, J. in *Cell: A Laboratory Manual* (eds Spector, D., Goldman, R. & Leinwand, L.) 108.101–108.109 (Cold Spring Harbor Laboratory Press, Cold Spring Harbor, 1998).

Acknowledgements

We acknowledge A. Puoti for providing the plasmid form of the cDNA library; R. Sternglanz, S. M. Hollenberg and A. Grimson for yeast strains and plasmids; and A. Steinberg and L. Vanderploeg for help with the illustrations. A.G.P. is an Howard Hughes Medical Institute predoctoral fellow. J.K. is an investigator of the Howard Hughes Medical Institute.

Correspondence and requests for materials should be addressed to J.K. (e-mail: jekimble@facstaff.wisc.edu). The mRNA sequences for *lag-3A* and *lag-3B* have been deposited in GenBank under accession codes AF241846 and AF241847, respectively.

Translocation step size and mechanism of the RecBC DNA helicase

Piero R. Bianco & Stephen C. Kowalczykowski

Sections of Microbiology and of Molecular and Cellular Biology, University of California at Davis, Davis, California 95616, USA

DNA helicases are ubiquitous enzymes that unwind double-stranded DNA^{1–3}. They are a diverse group of proteins that move in a linear fashion along a one-dimensional polymer lattice—DNA—by using a mechanism that couples nucleoside triphosphate hydrolysis to both translocation and double-stranded DNA unwinding to produce separate strands of DNA. The RecBC enzyme is a processive DNA helicase that functions in homologous recombination in *Escherichia coli*; it unwinds up to 6,250 base pairs per binding event and hydrolyses slightly more than one ATP molecule per base pair unwound. Here we show, by using a series of gapped oligonucleotide substrates, that this enzyme translocates along only one strand of duplex DNA in the 3' → 5' direction. The translocating enzyme will traverse, or 'step' across, single-stranded DNA gaps in defined steps that are 23 (±2) nucleotides in length. This step is much larger than the amount of double-stranded DNA that can be unwound using the free energy derived from hydrolysis of one molecule of ATP, implying that translocation and DNA unwinding are separate events. We propose that the RecBC enzyme both translocates and unwinds by a quantized, two-step, inchworm-like mechanism that may have parallels for translocation by other linear motor proteins.

DNA unwinding by RecBC enzyme initiates only at blunt or nearly blunt double-stranded DNA (dsDNA) ends; thus, it had not been possible to determine on which strand of DNA translocation occurs, or whether both DNA strands are required. We therefore

devised a strategy to determine both the polarity of and the step size for translocation. We first introduced a series of defined-size gaps in one or the other strand of otherwise duplex DNA, and then determined which size single-stranded DNA (ssDNA) gap prevented traversal. We used two types of substrates, each with a double-stranded blunt-end entry site at the 'proximal' 25-mer, an ssDNA gap, a 'tester' oligonucleotide (the 20-mer) distal to the gap and an ssDNA tail downstream of the annealed 20-mer (Fig. 1). The tail limits entry to only the dsDNA end; the gap is used to define the importance of that DNA strand in helicase translocation; and the displacement of the distal, tester oligonucleotide reports translocation and unwinding past the gap. Substrate set A has gaps positioned in the 5'-terminated strand relative to the entry point of the enzyme (the bottom strand of the substrates as shown), and substrate set B has gaps positioned in the 3'-terminated strand relative to the entry point of the enzyme (the top strand as shown). Gaps were initially either 0 (a nick) or 30 nucleotides (nt) in size (Fig. 1). A gap size of 30 nt was selected, as this is 9 nt larger than the contact length of the stationary holoenzyme bound to a dsDNA end⁴.

We reasoned that the translocating enzyme should dissociate from the substrate when it encounters a discontinuity larger than its contact length in a strand of DNA that is critical to translocation. If the enzyme translocates along only one strand of DNA, then it

should fail to bypass a gap present in that strand but not the other; if the enzyme requires both strands of DNA for translocation, then it should fail to bypass a gap (larger than its contact length) present in either strand. Failure to bypass a gap would be observed as formation of an intermediate unwinding product, consisting of the 100-mer (or alternatively the 130-mer) with the tester 20-mer distal to the gap, still bound.

When gaps of either 0 or 30 nt are present in the bottom strand, RecBC enzyme unwinds the substrate, displacing both the 25-mer proximal to the gap and the 20-mer downstream (Fig. 1a). This is observed as the disappearance of substrate in a time-dependent manner concomitant with the production of 100-mer ssDNA. Furthermore, displacement of both oligonucleotides is simultaneous (data not shown) with little or no intermediate species produced for either of these substrates, showing that a second RecBC enzyme is not responsible for displacement of the distal oligonucleotide. In the presence of single-stranded DNA binding (SSB) protein, RecBC enzyme cannot unwind substrates with only the internal 20-mers bound to the 100-mer (that is, substrates with a ssDNA tail at each end), showing that the enzyme requires the proximal dsDNA region to mediate unwinding beyond the gap (data not shown). Thus, RecBC enzyme is able to bypass gaps present in the 5'-terminated, or bottom strand, with more than 92% efficiency.

When gaps are positioned in the 3'-terminated strand, however, the results are significantly different (Fig. 1b). For the 0-nt-gap substrate, the enzyme can unwind and displace both the proximal 25-mer and the distal 20-mer; no intermediate is produced and ~65% of the starting substrate is converted to 100-mer in 2 min. In contrast, for the 30-nt-gap substrate the enzyme can displace only the proximal 25-mer; the 20-mer distal to the gap is not displaced efficiently, a significant amount of intermediate species accumulates (~55%), and the amount of 100-mer produced is decreased (down from 65% to 16%). Thus, RecBC enzyme is unable efficiently to bypass a 30-nt gap when that gap is present in the 3'-terminated, or top strand.

Identical results were obtained using single-round kinetic experiments in which the enzyme was pre-bound to the dsDNA end, and the reactions were initiated with a mixture of ATP and heparin (data not shown). Heparin prevents re-binding of RecBC enzyme after it has dissociated from a DNA molecule (ref. 5; and data not shown). Thus, the ability of the enzyme to bypass the 30-nt gap in the bottom strand (versus the top strand) is not owing to dissociation of

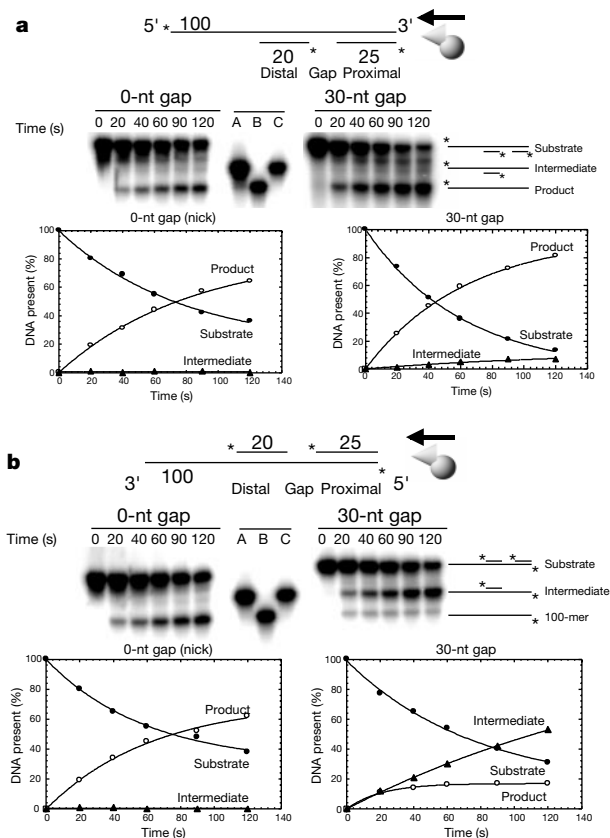


Figure 1 The RecBC helicase translocates in the 3' → 5' direction. Time courses of unwinding reactions using substrates with gaps present in the 5'-terminated (bottom) strand (**a**) and in the 3'-terminated (top) strand (**b**) are shown. The substrate for each reaction is shown above the gel. RecBC enzyme must translocate from right to left as shown (arrow); displacement of the oligonucleotide distal to the gap (20-mer) requires both displacement of the oligonucleotide proximal to the gap (25-mer) and traversal through the gap. The positions of substrate (filled circles), intermediate (triangles) and 100-mer product (open circles) are indicated to the right of each gel. Lanes A, B and C are standards: A, intermediate for the nicked substrate; B, 100-mer product; C, the intermediate for the 30-nt gap.

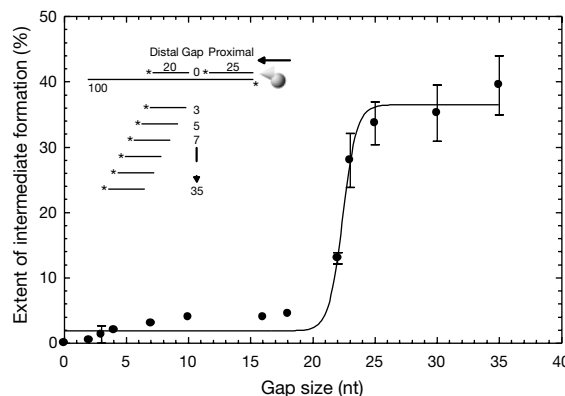


Figure 2 The observed step size for the translocating RecBC enzyme is 23 (±2) nucleotides. A compilation of the extents of intermediate formation from two-minute time courses for the substrates with increasing gap lengths is shown. Inset shows the substrates, which consist of a 100-mer with a 25-mer annealed to the 5' end, and with various 20-mers annealed to different positions on the 100-mer. Reactions and data analyses were carried out as in Fig. 1.

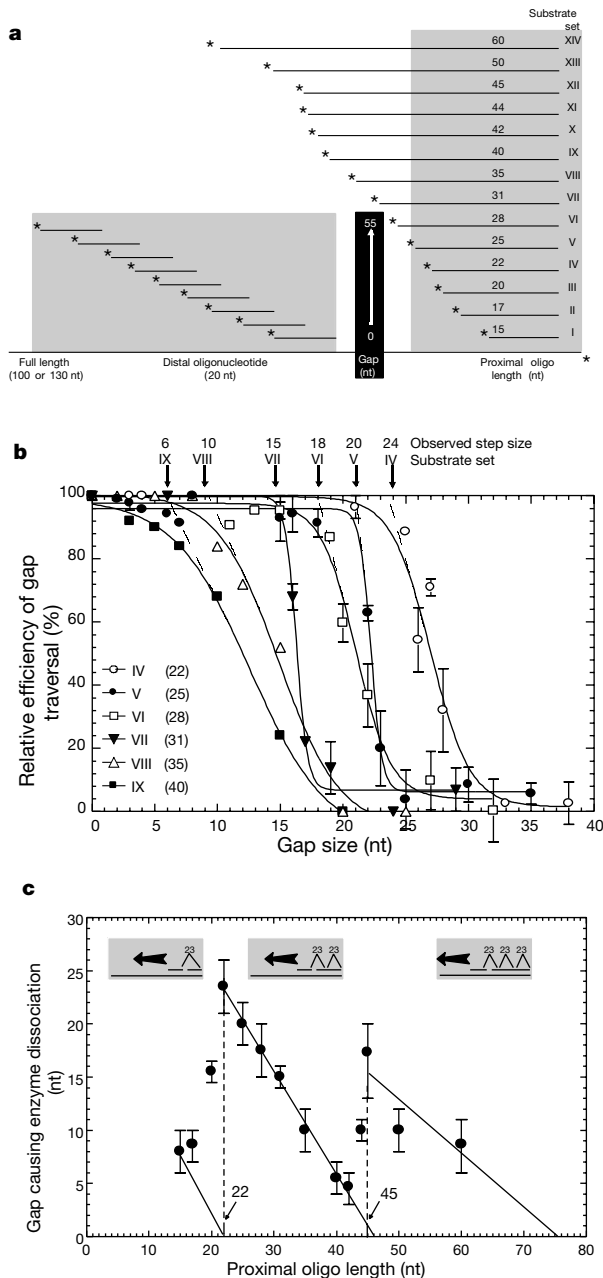


Figure 3 The observed step size is dependent on the length of the proximal duplex DNA region and displays a 23-nt periodicity for 3 cycles of translocation and DNA unwinding. **a**, Substrates. The arrangement of proximal and distal oligonucleotides bound to same 100-mer (or 130-mer) is shown. Thirteen additional substrate sets were constructed in identical fashion to those in Fig. 2 and are arranged according to the length of the oligonucleotide proximal to the gap (right grey box). In each set, the sequences of the 100-mer (or 130-mer, with 30 additional bases at the 3' end) and the set of 20-mers (left grey box) were always the same. The potential gap length generated is indicated (black box). **b**, Data compiled from helicase assays such as those shown in Fig. 2 using substrate sets IV–IX. Data are shown for a two-minute time point, averaged from two to seven assays, done on separate days for each substrate. For each substrate set, the extents were normalized to the average maximum extent of intermediate formation for that set: set IV, 56%; set V, 40%; set VI, 55%; set VII, 40%; and sets VIII and IX, 50%. Curves represent a fit to a sigmoid function (Prism v3.0, GraphPad Software) and were used to obtain the observed step size. Dashed lines and arrows indicate the observed step size for each data set (Table 1). Numbers in parentheses indicate the length of the proximal oligonucleotide. **c**, Compilation of data from helicase assays using substrate sets I–XIV. The gap causing enzyme dissociation for each substrate set (proximal oligonucleotide length) is the gap length at which the curves shown in **b** begin to decrease. Data for substrate sets I–III and X–XIV are not shown. Error bars represent the minimum and maximum value of the extrapolated step size. Grey boxes indicate the number of translocation steps taken by the helicase.

the enzyme at the gap followed by rapid re-binding with continued translocation. Furthermore, the inability to bypass gaps is not owing to a failure of RecBC enzyme to displace SSB protein bound in the gap, as similar results were obtained using the bacteriophage T4 gene 32 protein (data not shown). Collectively, these data show that, although it initiates by binding to dsDNA, RecBC enzyme requires only one strand of dsDNA for translocation (the strand 3' terminated at the entry end). Thus, RecBC enzyme translocates on this strand with 3' → 5' polarity.

Because the enzyme dissociates from the substrate when the strand on which it translocates has a gap of 30 nt, but not when the gap is a nick, this suggested a strategy to define the translocation step size of the enzyme. We reasoned that by varying the length of the gap in the 3'-terminated strand, we could determine the smallest gap size that the enzyme fails to bypass during translocation, and that this should correspond to the 'step size' for the enzyme. We therefore constructed a family of substrates with ssDNA gaps ranging from a nick to 35 nt (Fig. 2, inset).

Reactions and analyses identical to those in Fig. 1 were carried out for the substrates in Fig. 2. RecBC enzyme can bypass gaps up to 18 nt in size as determined by the low extents of intermediate formation. Above this gap size, the accumulation of intermediate increased ninefold to an average of 36% for gaps of 25 nt or bigger. Some RecBC enzymes may be able to traverse these larger gaps because of the inherent flexibility of the ssDNA regions in these gapped substrates; that is, the ssDNA in these gaps may 'loop out' bringing the two flanking dsDNA regions of the substrate into close proximity, thereby facilitating enzyme bypass. In any case, the sharp transition at 20–25 nt shows that translocation through such gaps is seriously impaired. Thus, these data show that when RecBC enzyme encounters gaps smaller than 22–23 nt, it can 'step across' them as though they were dsDNA, suggesting that the step size for the translocating enzyme is ~23 nt. In addition, these results imply the disposition of the DNA unwinding domain relative to the footprint of the enzyme: this domain must be positioned at or near the rear of the helicase for gap bypass to occur. If it were positioned at the front, then a gap in the translocating strand as small as 1 nt would function as a suicide substrate by causing the helicase to dissociate as a complex with the ssDNA that it had produced and released by DNA unwinding.

Such a large step size was unanticipated, as the largest unwinding step size reported to our knowledge for a DNA helicase is 4–5 nt (ref. 6). Furthermore, this translocation step size is much larger than the amount of DNA that can be unwound from the free energy derived from the hydrolysis of one molecule of ATP²⁷. To ensure that the failure of RecBC enzyme efficiently to bypass gaps of 23 (±2) nt or greater was not a consequence of the oligonucleotides used to construct the gap (because, for example, the sequence of the 20-mers following the gap is always different), additional substrate sets were constructed. For each set, the same 100-mer and family of distal 20-mers were used as for the substrates in Fig. 2, but the length of the oligonucleotide proximal to the gap was modified (Fig. 3a, substrate sets IV–IX). Thus, a gap of the same size would be present in each substrate set but the sequence of the oligonucleotides flanking that gap would be different. We expected that gap bypass should be the same in each of the six substrate sets, that is, ~23 nt.

Reactions and analyses were carried out using sets IV–IX; these data were converted to a 'relative efficiency of gap traversal' (Fig. 3b). Rather than being identical, each substrate set displays a distinctive curve. Unexpectedly, the gap-bypass efficiency decreases rapidly at a gap size that changes monotonically with each substrate set. Thus, the observed step size for the translocating RecBC enzyme appears to be dependent on the length of the proximal oligonucleotide (Table 1). This unexpected finding shows that the ability of RecBC helicase to traverse gaps as large as ~23 nt cannot be explained by proposing that the enzyme, with a static footprint of ~22 nt, simply positions itself across the gap so that the leading end

Table 1 Effects of proximal oligonucleotide length on gap bypass

Step cycle*	Substrate set	Proximal oligo length (nt)†	Observed step size (nt)‡	Total (nt)§	Inferred step size (nt) (mean = 23)
1	I	15	8	23	23
1	II	17	9	26	26
2	III	20	16	36	18
2	IV	22	24	46	23
2	V	25	20	45	23
2	VI	28	18	46	23
2	VII	31	15	46	23
2	VIII	35	10	45	23
2	IX	40	6	46	23
2	X	42	5	47	23
2	XI	44	10	54	27
3	XII	45	17	62	21
3	XIII	50	10	60	20
3	XIV	60	9	69	23

*Translocation step as shown in Fig. 3c.

†The length of the oligonucleotide proximal to the gap.

‡The observed step size corresponds to the gap at which the relative efficiency of gap traversal decreases below 100%.

§The total is the sum of the length of the oligonucleotide proximal to the gap and the observed step size.

||The inferred step size is equal to the total for sets I and II, and is obtained by dividing the total by 2 for sets III–XI and by 3 for sets XII–XIV (see text).

can bind the dsDNA across any ~23-nt gap. For such a model, in which the translocation step size is fixed relative to the end of the proximal dsDNA, RecBC enzyme should traverse any 23-nt gap, regardless of proximal dsDNA length. Thus, the data shown in Figs 2 and 3b argue against a model in which a motor domain at the rear of a fixed step-size helicase propels the leading edge of the protein across the gap where the leading domain can engage the duplex DNA, and thereby effect gap traversal. If this model were operative, then the gap size traversed should be a constant property (that is, 23 nt for all substrate sets) of the helicase.

The data in Table 1 (IV–IX) reveal that there is an inverse relationship between the size of the smallest gap that the enzyme fails to traverse, and the length of the oligonucleotide proximal to the gap. When these gap sizes are added to the length of the oligonucleotide proximal to the gap, a total length of 46 nt is obtained for each substrate set (column 4). This suggests that the step size is quantized and its length is determined relative to the entry point of RecBC enzyme into the dsDNA. In addition, the 3' end of the distal 20-mer is always 46 nt from the entry point when the blockage of translocation begins to occur. This implies either that the enzyme translocates with a step size of 46 nt, or that the step size is 23 nt and the enzyme fails to bypass the gap and dissociation occurs during the second step. The first interpretation is unlikely because the footprint of the holoenzyme enzyme is only 19 (±3) base pairs (bp) (ref. 4) and it functions as a single multimeric complex containing only one ATPase subunit^{8–10}. Furthermore, if the step size were 46 nt, then for all substrates where the sum of the proximal and distal oligonucleotides and the gap was less, neither of the oligonucleotides would be displaced, because in the first step the enzyme would step into a gap beyond the bound oligonucleotides and dissociate. Clearly, this is not the case. The second interpretation is more likely, which argues that the step size for RecBC enzyme is 23 nt (Table 1, IV–IX, right column).

To determine whether the step size remains constant during translocation, we constructed two additional groups of substrates. The first group used the shortest proximal oligonucleotides that could be reliably bound to the 100-mer: these were 15, 17 and 20 nt (I–III, Fig. 3a). The second group used longer proximal oligonucleotides (42, 44, 45, 50 or 60 nt; X–XIV) and required a 130-mer oligonucleotide instead of the 100-mer for substrate sets XII–XIV. We reasoned that if the step size remained constant throughout translocation, then the observed gap size traversed should display periodicity. It should approach a minimum at a proximal oligonucleotide length of ~23 nt, increase abruptly to ~23 and then decrease linearly over the span of ~23 nt, reaching a second

minimum at a proximal oligonucleotide length of ~46 nt, and so on. The results of helicase assays using these substrates clearly show a cyclic pattern (Fig. 3c), in which the gap-size traversed approaches a minimum, increases to 24 nt, decreases to a new extrapolated minimum at 46 nt, and then is followed by yet another sharp increase and another (partial) linear decline; that is, the cycle resets approximately every 23 nt. Thus, the step size of ~23 nt is constant for at least three cycles of translocation.

Our finding that RecBC enzyme can traverse ssDNA gaps smaller than 23 nt in length requires a mechanism to explain how a helicase can translocate with a step size of 23 despite being limited, thermodynamically, to no more than ~5 bp of unwinding per mole of ATP hydrolysed. To explain this potential dilemma, we propose a mechanism that we have termed the 'quantum inchworm' (Fig. 4), which is similar to a model proposed for *E. coli* RNA polymerase¹¹. In the quantum inchworm model, translocation and DNA unwinding are two separate, consecutive events: first, translocation occurs by a 23-bp 'step'; second, unwinding at the trailing domain occurs by several, smaller events of 2–5 bp for each ATP molecule hydrolysed. Consistent with the latter proposal, kinetic measurement of the DNA unwinding step size for RecBCD enzyme shows that it unwinds dsDNA in increments of 4–5 bp (A. Vindigni, personal communication). We propose that RecBC enzyme possesses two, non-equivalent DNA-binding sites: the first DNA-binding site is the leading domain of the enzyme that binds to one strand (the 3'-terminated strand) of dsDNA and functions to anchor the enzyme during DNA unwinding. The second DNA-binding site is the trailing domain that functions as the helicase domain of the enzyme and is responsible for separating the strands of DNA; this second domain must move in several smaller steps relative to the leading domain. We propose that one complete cycle of translocation and DNA unwinding is achieved by the expansion and contraction of the enzyme that includes the hydrolysis of at least 5 to 12 ATP molecules⁷.

The cycle (Fig. 4) begins with the enzyme bound to a dsDNA end (stage 1). The trailing domain is bound at the end and, consequently, the leading edge is positioned 23 nt from this end (23 bp in B-form dsDNA corresponds to ~7.8 nm). The leading domain anchors the enzyme in place by binding to only one strand of the DNA duplex (indicated by the hands wrapping around one strand of the duplex). The trailing domain unwinds the dsDNA behind the

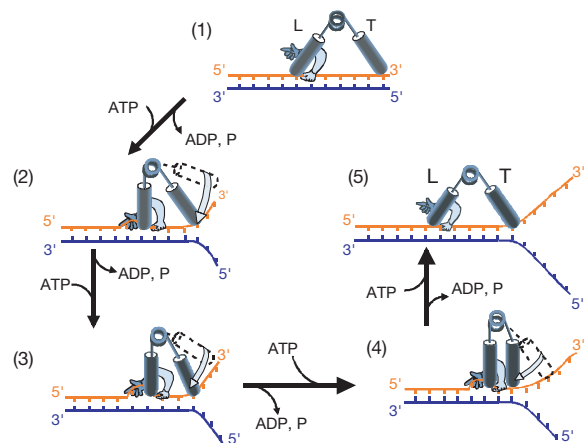


Figure 4 The RecBC enzyme translocates by a 'quantum inchworm' mechanism. A single catalytic cycle of translocation and DNA unwinding is shown. The individual strands of the DNA duplex are coloured orange (3'-terminated strand) and blue (5'-terminated strand). Translocation is from right to left along only one strand (3'-terminated) of the duplex. The enzyme contains two domains: a leading domain (L, which anchors the enzyme to only one strand of duplex DNA) and a trailing domain (T, responsible for DNA unwinding). The leading domain binds 23 nt ahead of the trailing domain.

leading edge, using the energy derived from ATP binding/hydrolysis both to separate the DNA strands and to advance with 4–5-bp steps toward the leading domain (stages 2–4). As the lagging domain translocates up to the leading domain (stage 4), a signal (yet to be determined) is transmitted from the lagging to the leading domain causing the leading domain to dissociate and rebind ~23 nt ahead of the bound lagging end (stage 5). The enzyme has now returned to the starting point and the cycle repeats itself until the DNA molecule is completely unwound or the enzyme dissociates. As the lagging domain approaches the anchored leading domain, torsional stress will accumulate in the intervening dsDNA. Because the trailing end of the enzyme must transiently disengage to advance, any accumulated torsional stress in the DNA could be released at this point, and, provided that the trailing end rapidly engages before the strands fully re-anneal, helicase function will remain processive as long as the leading end remains attached. One might expect to see an occasional uncoupling of unwinding and translocation (for example, the DNA strands partially re-anneal before the trailing end engages; this would result in an ‘inefficiency’ in ATP utilization. In fact, such an inefficiency is observed: for RecBC enzyme, as many as 1.4 ATP molecules are hydrolysed per base pair unwound¹², whereas for RecBCD enzyme 2–3 ATP molecules are hydrolysed per base pair unwound⁷; this is between 3–15-fold more hydrolysis than the minimum required of 0.2 ATP molecules hydrolysed per base pair unwound. Therefore, at most, only 1 of 3 hydrolytic events results in DNA unwinding, and the value may be as few as 1 of 15 events being productive. Thus, anchoring of the helicase to DNA by the leading domain gives the trailing unwinding domain multiple opportunities to act on its substrate without macroscopic dissociation.

The large conformational changes proposed are not without precedent. The crystal structures of the *Bacillus stearothermophilus* PcrA helicase^{13,14} and the *E. coli* Rep helicase¹⁵ have been determined. PcrA helicase was proposed to function as an inchworm¹⁶, as was the related UvrD helicase¹⁷. Our mechanism has parallels to those proposed for these helicases and, thus, we conclude that a similar underlying mechanism may be used by at least a subset of the linear motor proteins to perform mechanical work. □

Methods

Substrate construction

Oligonucleotides used for substrate construction were purified using denaturing polyacrylamide gels. The sequence of the 130-mer is 5′-TGGCCTGCAACGCGGGCATCCCCGATGCGCCGGAAGCGAGAAGAATCATAATGGGGGAAGGCCACCGCCTCGCGT CGCGAACCCAGCAAGACGTAGCCAGCGCGTGGCCGCCATGCCGGCGAT AATG-3′; the 100-mer lacked the last 30 nt. Oligonucleotide concentrations were determined using an extinction coefficient calculated for each oligonucleotide. Oligonucleotides were labelled at the 5′ ends using T4 polynucleotide kinase and γ -³²P-ATP. Annealing was performed in T4 polynucleotide kinase buffer plus 10 mM magnesium acetate containing the 100- (or 130-), 25- and 20-mers at a ratio of 100-mer:25-mer:20-mer of 1:1.1:1.2, to ensure that all of the 100-mer was converted to the substrate form. The mixture was heated to 100 °C for 5 min, and allowed to cool to room temperature. Substrate formation was confirmed by electrophoresis. Typically, 100% of the 100-mer was converted to substrate; the SSB protein bound the residual 25- and 20-mer.

Assay system

Helicase assays were conducted at room temperature and contained 25 mM Tris-HCl pH 7.5, 1 mM dithiothreitol, 8 mM magnesium acetate, 1 mM ATP, 1 μ M SSB, 10 nM DNA (in mol of 100-mers) and 1.03 nM active RecBC enzyme. SSB protein ensures entry from the blunt end of the DNA, and prevents re-annealing of unwound strands. For single-round experiments, RecBC helicase was bound to DNA for 2 min and reactions were initiated by the addition of an ATP-heparin mix (1 mM and 10 mg ml⁻¹, final). Reactions were stopped by an equal volume of ficoll gel loading dye mix, containing SDS (1%, final), EDTA (50 mM) and proteinase K (0.4 mg ml⁻¹). After 5 min, aliquots were loaded onto polyacrylamide gels (1:1.5 bis:acrylamide in TBE buffer). After electrophoresis, the gels were analysed using a Molecular Dynamics Storm 840 and ImageQuaNT software.

Received 4 October; accepted 15 March 2000.

1. Matson, S. W., Bean, D. W. & George, J. W. DNA helicases: enzymes with essential roles in all aspects of DNA metabolism. *Bioessays* **16**, 13–22 (1994).
2. Lohman, T. M. & Bjornson, K. P. Mechanisms of helicase-catalyzed DNA unwinding. *Annu. Rev. Biochem.* **65**, 169–214 (1996).

3. West, S. C. DNA helicases: new breeds of translocating motors and molecular pumps. *Cell* **86**, 177–80 (1996).
4. Ganesan, S. & Smith, G. R. Strand-specific binding to duplex DNA ends by the subunits of *Escherichia coli* recBCD enzyme. *J. Mol. Biol.* **229**, 67–78 (1993).
5. Korangy, F. & Julin, D. A. Kinetics and processivity of ATP hydrolysis and DNA unwinding by the RecBC enzyme from *Escherichia coli*. *Biochemistry* **32**, 4873–4880 (1993).
6. Ali, J. A. & Lohman, T. M. Kinetic measurement of the step size of DNA unwinding by *Escherichia coli* UvrD helicase. *Science* **275**, 377–380 (1997); erratum, *ibid* **276**, 21 (1997).
7. Roman, L. J. & Kowalczykowski, S. C. Characterization of the adenosinetriphosphatase activity of the *Escherichia coli* RecBCD enzyme: Relationship of ATP hydrolysis to the unwinding of duplex DNA. *Biochemistry* **28**, 2873–2881 (1989).
8. Korangy, F. & Julin, D. A. A mutation in the consensus ATP-binding sequence of the RecD subunit reduces the processivity of the RecBCD enzyme from *Escherichia coli*. *J. Biol. Chem.* **267**, 3088–3095 (1992).
9. Taylor, A. F. & Smith, G. R. Monomeric RecBCD enzyme binds and unwinds DNA. *J. Biol. Chem.* **270**, 24451–24458 (1995).
10. Bianco, P. R. & Kowalczykowski, S. C. The recombination hotspot Chi is recognized by the translocating RecBCD enzyme as the single strand of DNA containing the sequence 5′-GCTGGTGG-3′. *Proc. Natl Acad. Sci. USA* **94**, 6706–6711 (1997).
11. Chamberlin, M. J. New models for the mechanism of transcription elongation and its regulation. *Harvey Lectures* **88**, 1–21 (1992).
12. Korangy, F. & Julin, D. A. Efficiency of ATP hydrolysis and DNA unwinding by the RecBC enzyme from *Escherichia coli*. *Biochemistry* **33**, 9552–9560 (1994).
13. Subramanya, H. S., Bird, L. E., Brannigan, J. A. & Wigley, D. B. Crystal structure of a DExx box DNA helicase. *Nature* **384**, 379–383 (1996).
14. Velankar, S. S., Soultanas, P., Dillingham, M. S., Subramanya, H. S. & Wigley, D. B. Crystal structures of complexes of PcrA DNA helicase with a DNA substrate indicate an inchworm mechanism. *Cell* **97**, 75–84 (1999).
15. Korolev, S., Hsieh, J., Gauss, G. H., Lohman, T. M. & Waksman, G. Major domain swiveling revealed by the crystal structures of complexes of *E. coli* Rep helicase bound to single-stranded DNA and ADP. *Cell* **90**, 635–647 (1997).
16. Bird, L. E., Subramanya, H. S. & Wigley, D. B. Helicases: a unifying structural theme? *Curr. Opin. Struct. Biol.* **8**, 14–18 (1998).
17. Mechanic, L. E., Hall, M. C. & Matson, S. W. *Escherichia coli* DNA helicase II is active as a monomer. *J. Biol. Chem.* **274**, 12488–12498 (1999).

Acknowledgements

We thank D. Anderson, R. Ando, D. Arnold, C. Barnes, R. Baskin, F. Chedin, F. Harmon, J. Kleiman, J. New, E. Seitz, and S. Shetterley for their comments. This work was supported by a grant from the NIH.

Correspondence and requests for materials should be addressed to S.C.K. (e-mail: sckowalczykowski@ucdavis.edu).

The crystal structure of the photoprotein aequorin at 2.3 Å resolution

James F. Head*, Satoshi Inouye†, Katsunori Teranishi‡ & Osamu Shimomura*§

* Structural Biology Group, Department of Physiology, Boston University School of Medicine, Boston, Massachusetts 02118, USA

† Yokohama Research Centre, Chisso Corporation, 5-1 Okawa, Kanazawa-ku, Yokohama 236, Japan

‡ Faculty of Bioresources, Mie University, Kamihama, Tsu 514, Japan

§ Marine Biologicals Laboratory, Woods Hole, Massachusetts 02543, USA

Aequorin is a calcium-sensitive photoprotein originally obtained from the jellyfish *Aequorea aequorea*¹. Because it has a high sensitivity to calcium ions and is biologically harmless, aequorin is widely used as a probe to monitor intracellular levels of free calcium. The aequorin molecule contains four helix–loop–helix ‘EF-hand’ domains, of which three can bind calcium². The molecule also contains coelenterazine as its chromophoric ligand³. When calcium is added, the protein complex decomposes into apoaequorin, coelenteramide and CO₂, accompanied by the emission of light⁴. Apoaequorin can be regenerated into active aequorin in the absence of calcium by incubation with coelenterazine, oxygen and a thiol agent⁵. Cloning and expression of the com-